Evaluation of a Small Cadmium Zinc Telluride Detector for Scintimammography

Bryon Mueller, PhD[1]; Michael K. O'Connor, PhD[1]; Ira Blevis, PhD[2]; Deborah J. Rhodes, MD[3]; Robin Smith, MD[3]; Douglas A. Collins, MD[1]; and Stephen W. Phillips, MD[1]

[1]Department of Radiology, Mayo Clinic, Rochester, Minnesota; [2]Functional Imaging, General Electric Medical Systems, Haifa, Israel; and [3]Department of Internal Medicine, Mayo Clinic, Rochester, Minnesota

The purpose of this study was to evaluate a small semiconductor-based gamma camera that may have applications in scintimammography. **Methods:** A small cadmium zinc telluride (CZT) detector was evaluated. The detector had a field of view of 20 × 20 cm with detector elements of 2.5 × 2.5 mm in size. Both short-bore (35 mm) and long-bore (50 mm) collimators, matched to the geometry of the detector elements, were evaluated. The imaging performance of the CZT detector was compared with that of a conventional gamma camera equipped with all-purpose and ultra-high-resolution collimators. The performance of both systems with respect to breast imaging was evaluated using a water tank containing small glass spheres, 1.8–9.8 mm in diameter. The effects of variations in breast thickness, tumor depth, and tumor-to-background ratio were all simulated in this phantom model. Total counts per image were adjusted to approximate the count density observed in clinical scintimammographic studies. **Results:** Sensitivity of the CZT detector was 76% that of the equivalent NaI system. The system demonstrated excellent integral uniformity. The energy resolution of the CZT system was 6.5% for ^{99m}Tc. Spatial resolution with the long-bore collimator was superior to that of a conventional large field-of -view gamma camera equipped with an ultra-high- resolution collimator, over the range 0–6 cm from the collimator face. A blinded review of breast phantom images showed that small spheres (≤7 mm in diameter) were better seen and had a better tumor-to-background ratio with the CZT system than with the conventional gamma camera. **Conclusion:** A small CZT detector offers superior performance to a conventional gamma camera and should permit reliable detection of breast tumors <1 cm in size.

Key Words: cadmium zinc telluride detector; scintimammography; breast

J Nucl Med 2003; 44:602–609

The quality of scintimammographic images obtained with a conventional Anger-based gamma camera is limited by several factors. The primary limitation is the inability to position the gamma camera close to the breast. Consequently, the breast must be imaged in the prone lateral position with poor visualization of lesions located in the medial wall or close to the chest wall. Optimal scintimammographic imaging requires a system that cannot only be positioned close to the breast but also allows the breast to be imaging from any side with minimal interference from adjacent activity in the body. Conventional Anger-based gamma cameras cannot be positioned in this manner because of the 8- to 10-cm dead space between the active area and the physical edge of the detector.

Several studies have reported on the development of small compact gamma-camera systems that overcome the problem of a large dead space. Several systems have been developed based on position-sensitive photomultipliers (PSPMTs) coupled to an array of NaI or CsI crystals (*1–3*). These systems generally have excellent spatial resolution close to the collimator face, which is important for breast imaging. However, most of these systems have significantly poorer energy resolution than Anger-based systems (*1,3*). An alternative to PSPMTs for light detection is a silicon photodiode usually coupled to CsI rather than NaI (*4,5*). These systems have achieved energy resolutions of 8%–10%, which are comparable to those obtained with Anger-based systems. Some PSPMT-based systems have been developed using a single NaI crystal (*2,6*). These systems have better energy resolution than the multicrystal systems but a very small field of view (6 × 6 cm), making them impractical for patient studies.

As an alternative to the above systems, over the last 5 y considerable progress has been made in the development of room temperature semiconductor– based gamma cameras (*7–9*). These systems have <1-cm dead space at the edge of the field of view and their modular nature permits detectors of any size to be constructed. From a performance perspective, these systems have similar spatial resolution to PSPMT and silicon photodiode– based systems, but significantly better energy resolution. Butler et al. (*8*) reported an energy resolution of <4% for ^{99m}Tc. With close proximity to the breast coupled with improved energy and spatial resolution, cadmium zinc telluride (CZT)–based gamma cameras should be able to detect smaller breast tumors than can be detected with conventional Anger-based systems.

Received Jul. 22, 2002; revision accepted Nov. 27, 2002.
For correspondence or reprints contact: Michael K. O'Connor, PhD, Section of Nuclear Medicine, Charlton 1-225, Mayo Clinic, Rochester, MN 55905.
E-mail: mkoconnor@mayo.edu

The purpose of this study was to evaluate a small CZT gamma camera both in terms of its performance characteristics and its application to scintimammography.

MATERIALS AND METHODS

CZT Detector

The CZT gamma camera evaluated in this study (Fig. 1) was a laboratory prototype (General Electric Medical Systems, Haifa, Israel). The detector contained 25 CZT modules. Each module was 4 × 4 cm with 256 (16 × 16) CZT elements per module, giving an 80 × 80 array of CZT elements. Each element had dimensions of 2.5 × 2.5 mm with a thickness of 5 mm. The 80 × 80 array had a total detector area of 20 × 20 cm^2. The system had a useful energy range of 50–200 keV and was equipped with either a general-purpose (GP) or a long-bore (LB) collimator. The collimators had square holes with dimensions of 2.3 × 2.3 × 35 mm and 2.3 × 2.3 × 50 mm for the GP and LB collimators, respectively. The collimator holes were matched to the geometry of the detector elements. System sensitivity was measured for both collimators using a point source of ^{99m}Tc placed at 10 cm from the collimator face and a −8%/+10% energy window centered on the 140-keV photopeak of ^{99m}Tc.

System uniformity was measured using a refillable ^{99m}Tc sheet source. Integral and differential uniformity values were determined according to the National Electrical Manufacturers Association standard (*10*). To determine system stability, measurements were performed over a period of 40 d without intervening recalibration of the system. Energy resolution was measured intrinsically from the full width at half maximum of the photopeak using point sources of ^{99m}Tc and ^{57}Co. Extrinsic spatial resolution was measured using a ^{99m}Tc line source placed at distances of 0.5–10 cm from the collimator face. The line source was orientated at a precisely known oblique angle to the collimator holes to permit oversampling of the pixels. Count profiles of the line source images were generated and the full width at half maxima were measured. Linear regression analysis was used to determine the relationship between distance and extrinsic resolution. All images were acquired in an 80 × 80 matrix size with a pixel size of 2.5 × 2.5 mm. For convenience, this matrix was padded out to a 128 × 128 matrix with blank pixels.

FIGURE 1. CZT detector with compression paddle mounted on stand for scintimammography.

Gamma Camera

To compare the CZT detector with a conventional gamma camera, procedures comparable to those described above were performed on 1 head of a standard dual-head gamma camera (Helix system; Elscint, Haifa, Israel). This system was equipped with either a GP (HPC-35) or ultra-high resolution (HPC-46) collimator. The collimators had hexagonal holes of diameter 2.0 and 2.7 mm and length 35 and 38 mm for the HPC-46 and HPC-35 collimators, respectively. System sensitivity was measured for both collimators using a standard 20% energy window centered on the 140-keV photopeak of ^{99m}Tc. In addition, system sensitivity was measured for the GP CZT collimator on the Helix system by removing the Helix collimator and placing the CZT collimator on the crystal. The parts of the crystal that were left exposed were shielded with lead. All images were acquired into 128 × 128 matrix size with a zoom of 2, giving a pixel size of 2.2 mm. Extrinsic spatial resolution was measured using a ^{99m}Tc line source placed at distances of 5–20 cm from the collimator face and aligned along the *x*- or *y*-axis of the gamma camera. Count profiles of the line source images were generated and the full width at half maxima were measured. Linear regression analysis was used to determine the relationship between distance and extrinsic resolution.

Breast Phantom

A breast phantom (Fig. 2) was constructed to evaluate the expected performance of this system in scintimammography. This comprised a 20 × 20 × 20 cm plastic box containing a small plastic jig on which 3 glass rods containing 4 spheres each were mounted to simulate breast tumors. On each rod, the spheres were constructed to have approximate diameters of 10, 7.5, 5, and 2.5 mm. Actual measured internal diameters of the 12 spheres were 9.8, 9.3, 9.2, 7.2, 7.2, 6.7, 4.9, 4.6, 4.4, 3.2, 2.2, and 1.8 mm. Breast thickness, tumor depth, and the ratio of tumor to soft-tissue activity were all adjustable in this phantom. For this study, breast thickness was varied from 3 to 6 cm. This range closely matches that seen in clinical scintimammographic studies with light (pain free) compression, where breast thickness in the craniocaudal view averaged 4.6 ± 2.9 cm and only 6% of breasts had a thickness of >6 cm (*11*). "Tumor" depth was varied from 1 to 4 cm. The phantom and spheres were filled with water and ^{99m}Tc to give tumor-to-background (T/B) ratios of 3:1, 6:1, and 12:1. This range of T/B ratios corresponds to those observed in patients with breast cancer, where the average ratio of tumor to soft-tissue from postoperative tissue samples ranged from approximately 2:1 to 13:1, with a mean value of 5.64 ± 3.06 (*12*).

Acquisition Parameters

To determine the appropriate count density that would simulate clinical studies, we analyzed 25 scintimammographic studies acquired on a conventional gamma camera (Orbiter 7500; Siemens

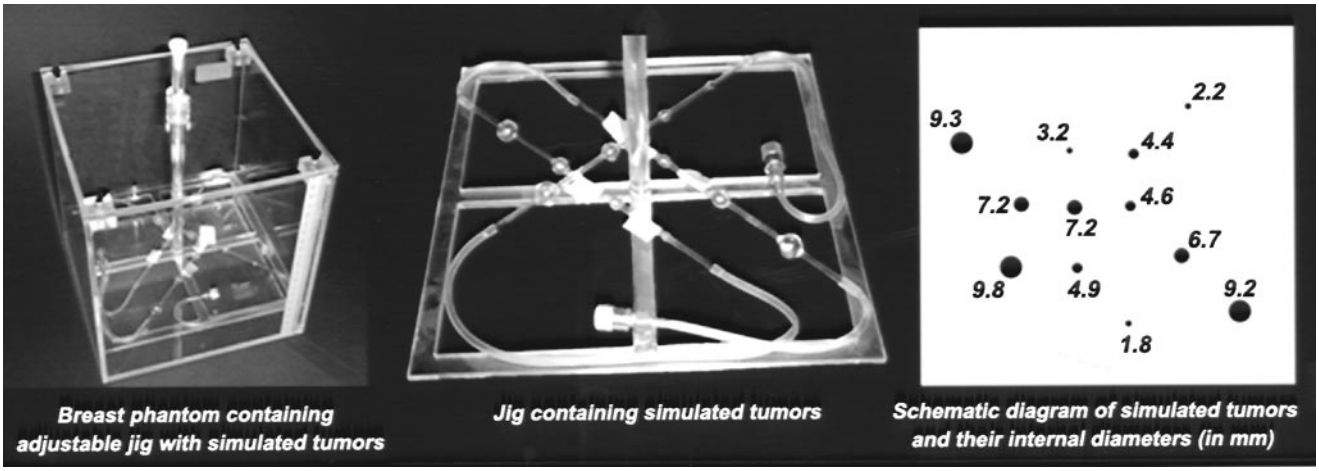

FIGURE 2. Breast phantom with plastic jig supporting array of simulated tumors (9.8–1.8 mm in diameter). Schematic diagram shows size and location of simulated tumors.

Medical Systems, Hoffman Estates, IL) equipped with a high-resolution collimator (collimator sensitivity was measured at 6.08 counts [cts]/min/kBq). After injection of 1.11 GBq (30 mCi) ^{99m}Tc-sestamibi, lateral views of the breast were acquired for 10 min per view. Using region-of-interest analysis, counts in each breast were obtained and adjusted for region size to give counts/cm^2. The average count density (in counts/cm^2) was obtained for all 25 studies and multiplied by a factor of 400 to give the total counts that would be acquired if the breast were to occupy fully a 20 × 20 cm field of view. This value was adjusted to account for differences in collimator sensitivity on the CZT and Helix systems. All breast phantom images on the CZT and Helix systems were acquired for their respective adjusted total counts.

From images acquired with the GP (CZT) and HPC-35 (Helix) collimators, 4 observers scored the number of tumors seen in the breast phantom images for various breast thicknesses and T/B ratios. In detail, 1 image was acquired at each of 3 breast thicknesses, 3.0, 4.5, and 6.0 cm, for tumors at a depth of 2 cm with a T/B ratio of 6:1 (3 CZT images, 3 Helix images). Likewise, 1 image was acquired at each T/B ratio, 3:1, 6:1, and 12:1, for tumors at a depth of 2 cm in a 4.5-cm-thick breast (3 CZT images, 3 Helix images). Each observer reviewed the 12 images with 12 tumors present in each image. To blind observers to tumor location, each image was modified in Photoshop (Version 6.0; Adobe Inc., San Jose, CA), and tumors were randomly repositioned throughout the image. Tumor detection was ranked on a 1–5 scale (5 = focal uptake, high intensity; 4 = focal uptake, medium intensity; 3 = focal uptake, low intensity; 2 = equivocal uptake; 1 = normal, no tumor). To improve the statistical accuracy of the results, data were pooled for tumors of the same approximate size, resulting in 4 groups with average diameters of 9.4 ± 0.3, 7.0 ± 0.3, 4.6 ± 0.2, and 2.4 ± 0.7 mm. For each group, the average score per reviewer was calculated. T/B contrast in these images was determined by measuring the maximum pixel value within a small region of interest placed over each lesion (or its known location if not clearly visible) and dividing by the mean background pixel value.

To illustrate clinical image quality, examples of 2 patient studies are presented in the Results. Studies were performed 10 min after injection of 740 MBq (20 mCi) ^{99m}Tc-sestamibi. Craniocaudal (or reverse craniocaudal) and mediolateral oblique views were obtained of each breast for 10 min per view using the LB collimator.

RESULTS

Performance Characteristics

For ^{99m}Tc, the energy resolution was measured at 6.5% and 8.7% for the CZT and Helix systems, respectively. Figure 3 shows comparable intrinsic energy spectra from the CZT and Helix systems for a point source of ^{57}Co. The conventional gamma camera does not yield the clear separation of the 122- and 136-keV photopeaks seen in the spectrum from the CZT detector. However, the CZT spectrum shows increased counts below the photopeak due to the tailing phenomena associated with semiconductor detectors (*7*).

Several defective CZT pixels were present in this prototype system. These pixels showed up as cold spots on the

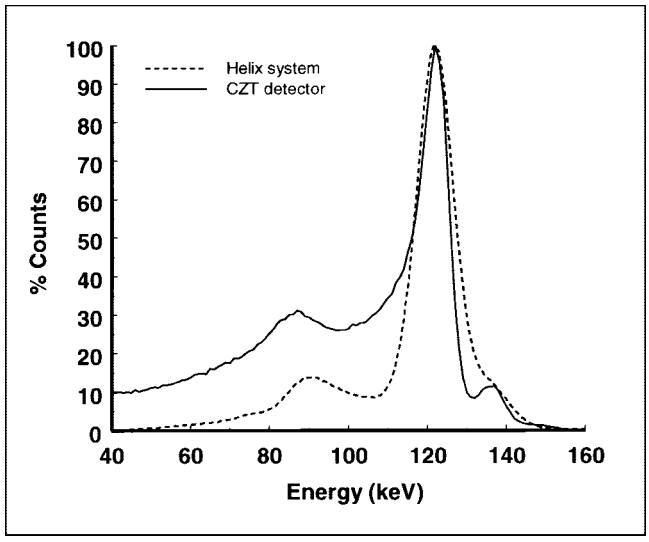

FIGURE 3. Energy spectra for ^{57}Co from CZT and Helix gamma cameras.

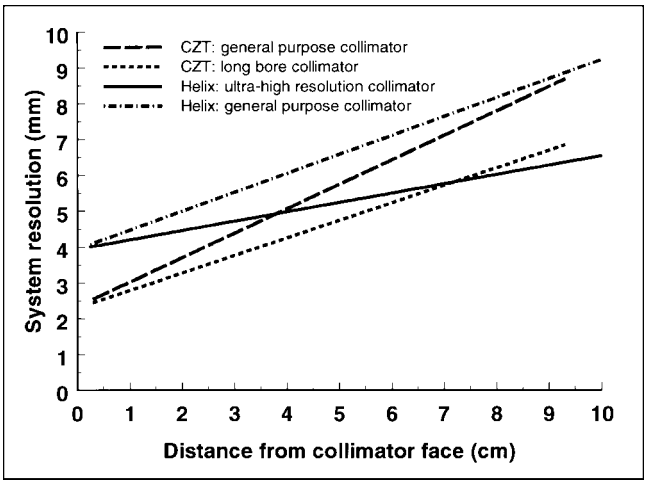

FIGURE 4. Collimator resolution as function of distance from collimator face for GP and LB collimators on CZT system and for HPC-35 (GP) and HPC-46 (ultra-high resolution) collimators on Helix system.

uniformity images. For measurement of uniformity, these pixels were excluded and replaced by their nearest-neighbor averages. System uniformity degraded slightly over the 40-d evaluation period, from an integral uniformity of 2.0% on day 1 to ~3% on day 40. Likewise, energy resolution showed a small change over this period (6.5% on day 1 and 6.8% on day 40).

Measured collimator sensitivities for the CZT detector were 7.30 cts/min/kBq and 3.05 cts/min/kBq for the GP and LB collimators, respectively. For the Helix gamma camera, measured collimator sensitivities were 7.43 cts/min/kBq and 2.95 cts/min/kBq for the GP (HPC-35) and ultra-high-resolution (HPC-46) collimators, respectively. Measurement of the sensitivity of the GP CZT collimator on the Helix system yielded a value of 9.60 cts/min/kBq, indicating a detection efficiency of 76% for the CZT detector relative to the Helix system. Hence, because comparable system sensitivities were obtained between the CZT detector with the LB collimator and the Helix system with the ultra-high-resolution collimator, it can be assumed that the LB collimator had poorer collimator resolution than the HPC-46 collimator. This is confirmed (Fig. 4). Figure 4 plots the measured system resolution for the GP and LB collimators on the CZT detector compared with the measured system resolution for the GP (HPC-35) and high-resolution (HPC-46) collimators on the Helix system. At the clinically relevant tumor depths of 2–4 cm, the LB collimator yields a 0.8- to 1.2-mm improvement in system resolution relative to the HPC-46 collimator, with comparable sensitivity, whereas the GP collimator yields up to 0.8-mm improvement in resolution with a factor of 2.5 increase in sensitivity. These gains in resolution are primarily due to matching of the CZT elements to the collimator holes, because this effectively eliminates the impact of intrinsic resolution on system resolution. It is only at distances of >7 cm that the ultra-high-resolution collimator on the Helix system exceeds the performance of the LB collimator on the CZT detector.

Breast Phantom Results

Analysis of the count density in the 25 clinical scintimammograms gave an average value of 4.56 ± 2.56 kcts/cm^2. This corresponds to 1.8 Mcts for a 20 × 20 cm breast phantom. Acquired total counts per image on the CZT detector were adjusted to 2.16 and 0.90 Mcts for the GP and LB collimators, respectively. Corresponding values for the HPC-35 and HPC-45 collimators on the Helix system were 2.2 and 0.87 Mcts, respectively.

Figure 5 shows comparable images of the breast phantom acquired on the CZT and Helix systems with both GP and high-resolution collimators. The T/B ratio was 6:1 with a tumor depth of 2 cm in the 4.5-cm-thick breast and 3 cm in the 6-cm-thick breast. Because the use of the higher resolution collimators (LB and HPC-46) appeared to give comparable results in terms of tumor contrast to those obtained with the GP collimators, further studies on the CZT and Helix systems were performed using the GP and HPC-35 collimators, respectively.

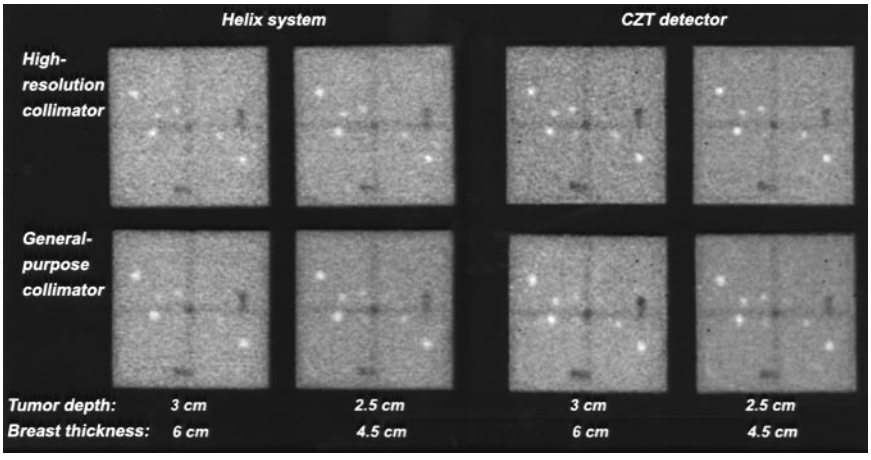

FIGURE 5. Images of breast phantom acquired on CZT and Helix systems with general-purpose and high-resolution collimators. Images were acquired at tumor depths of 3 and 2.5 cm with breast thickness of 6 and 4.5 cm, respectively. T/B ratio = 6:1 for all images.

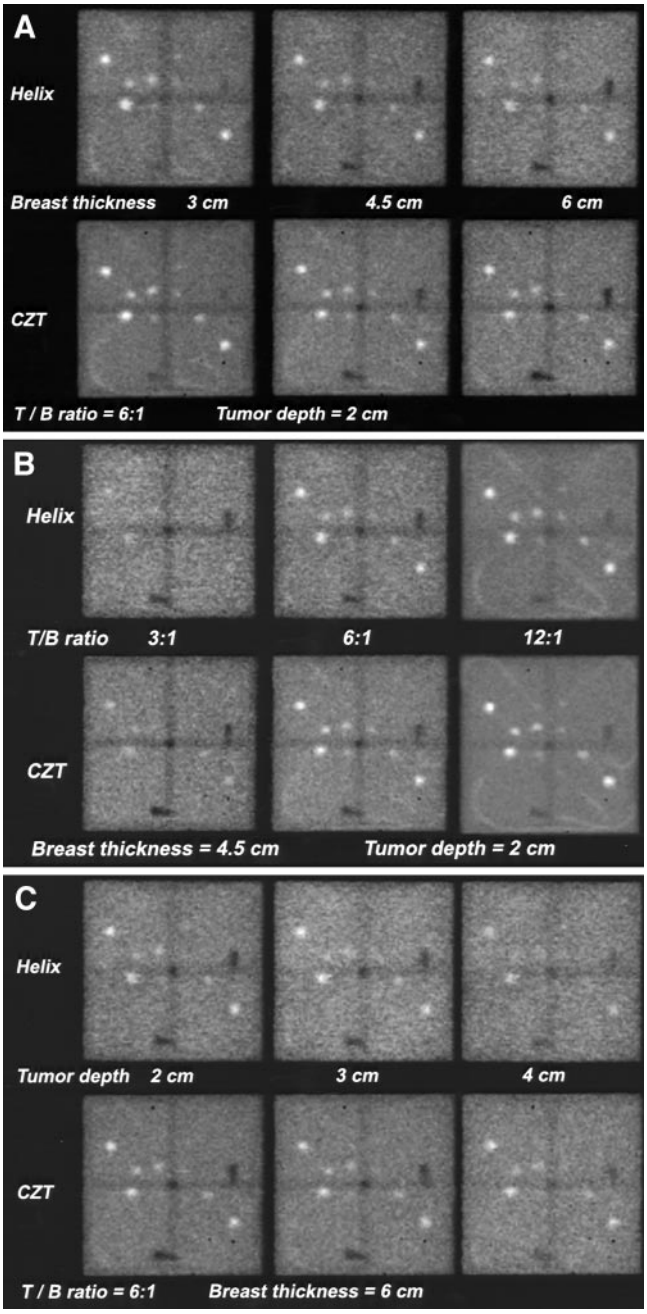

FIGURE 6. Comparison of images of breast phantom acquired on CZT and Helix systems with general-purpose collimators. (A) Effect of breast thickness on tumor visibility. Images were acquired at tumor depth of 2 cm with breast thickness of 3–6 cm. T/B ratio = 6:1 for all images. (B) Effect of T/B ratio on tumor visibility. Images were acquired at tumor depth of 2 cm with breast thickness of 4.5 cm. T/B ratio ranged from 3:1 to 12:1. (C) Effect of tumor depth on tumor visibility. Images were acquired at tumor depths of 2–4 cm with breast thickness of 6 cm. T/B ratio = 6:1 for all images.

Figure 6 shows the effect of breast thickness, tumor depth, and T/B ratio on the visibility of tumors in the breast phantom with the CZT and Helix systems equipped with the GP collimators. Of these 3 variables, the T/B ratio appears to have the most significant effect on tumor detection. Tables 1–4 compare tumor score and tumor contrast on the CZT and Helix systems as a function of average tumor diameter for various T/B ratios and breast thicknesses. Whereas tumor score was comparable between the CZT and Helix systems for tumors 9–10 mm in diameter, the CZT system had consistently higher scores for tumors ≤7 mm in diameter at all T/B ratios and breast thicknesses. Likewise, with the exception of the smallest (<4 mm) tumors, contrast was higher in the CZT images compared with the Helix images at all T/B ratios and breast thicknesses.

TABLE 1
Effect of Breast Thickness on Average Tumor Score

Breast thickness (cm)	Tumor diameter			
	9.4 mm	7.0 mm	4.6 mm	2.6 mm
6.0	5.0/5.0	4.2/3.7	1.4/1.1	1.0/1.0
4.5	5.0/5.0	4.3/3.8	2.4/1.2	1.0/1.0
3.0	5.0/5.0	4.8/4.7	3.0/1.4	1.0/1.0

Tumor depth = 2 cm; T/B ratio = 6:1. Results are shown for CZT/Helix systems for each breast thickness and average tumor diameter.

Figure 7 shows 2 examples of clinical ^{99m}Tc-sestamibi breast studies acquired on the CZT system (craniocaudal views). Surgical pathology confirmed the presence of 10.6- and 5-mm infiltrating ductal carcinomas in these patients.

DISCUSSION

This prototype CZT detector illustrates many of the advantages a semiconductor-based gamma camera has over a conventional Anger-based gamma-camera system. Semiconductor-based systems have significantly better energy resolution than Anger-based systems (Fig. 3) or multicrystal NaI or CsI systems using PSPMTs or silicon photodiodes (*1–6*). The pixilated nature of this detector results in an intrinsic resolution of 2.5 mm. Because the collimator is matched to the individual detector elements, the system resolution is effectively determined solely by the collimator resolution. With a conventional gamma camera, the colli-

TABLE 2
Effect of Breast Thickness on Tumor Contrast

Breast thickness (cm)	Tumor diameter			
	9.4 mm	7.0 mm	4.6 mm	2.6 mm
6.0	1.59/1.53	1.41/1.30	1.20/1.20	1.14/1.16
4.5	1.76/1.68	1.44/1.36	1.23/1.21	1.16/1.20
3.0	2.04/1.95	1.61/1.54	1.33/1.29	1.15/1.23

Tumor depth = 2 cm; T/B ratio = 6:1. Results are shown for CZT/Helix systems for each breast thickness and average tumor diameter.

TABLE 3
Effect of T/B Ratio on Average Tumor Score

T/B ratio	Tumor diameter			
	9.4 mm	7.0 mm	4.6 mm	2.6 mm
3:1	4.3/3.7	1.7/1.5	1.0/1.0	1.0/1.0
6:1	5.0/5.0	4.3/4.0	1.4/1.0	1.0/1.0
12:1	5.0/5.0	5.0/5.0	3.6/3.4	1.5/1.1

Tumor depth = 2 cm; breast thickness = 4.5 cm. Results are shown for CZT/Helix systems for each T/B ratio and average tumor diameter.

mator and the crystal are 2 independent devices, each with their own resolving power. Hence, if multiple γ-rays enter through the same hole in the collimator and strike exactly the same spot on the crystal, the limited resolution of NaI further degrades the positioning of these events by 3–4 mm. However, with pixilated detectors, if each collimator hole is matched to an individual pixel element, the collimator hole + pixel element can be considered as an independent detector relative to adjacent collimator holes; hence, resolution is determined only by the collimator. This can be seen from Figure 4, where the system resolution with CZT at 0 cm is 2.5 mm—the width of the collimator hole—whereas with the Helix system it is 4 mm (collimator resolution, 2 mm; intrinsic resolution, 3.5 mm). Hence, there is a significant gain in system resolution at distances of 0–6 cm from the collimator face compared with a conventional NaI-based system (Fig. 4).

In addition to its superior performance characteristics, the CZT detector is a more compact detector, with a thickness of ~5 cm compared with a thickness of 30–40 cm for a conventional system. This allows for a significant reduction in detector shielding and weight and should permit the design of imaging systems that are more compact and lightweight. An additional advantage that is discussed in more detail below is the absence of a large dead space at the edge of the detector field of view. The modular nature of the CZT detector also permits the fabrication of detectors in a variety of shapes and sizes. These physical features of the CZT detector permit it to be used in ways not possible with a conventional system. It can be used to image the breast in a similar manner to conventional mammography. It can be positioned closer to the body for lymphoscintigraphy than a conventional system, and a smaller version would be of value for intraoperative surgical procedures. It should also be noted that the system evaluated in this study was a prototype and we anticipate improvements in many of its performance characteristics as this technology matures.

TABLE 4
Effect of T/B Ratio on Tumor Contrast

T/B ratio	Tumor diameter			
	9.4 mm	7.0 mm	4.6 mm	2.6 mm
3:1	1.27/1.32	1.21/1.19	1.15/1.19	1.16/1.22
6:1	1.76/1.68	1.44/1.36	1.23/1.21	1.16/1.20
12:1	2.63/2.48	1.83/1.78	1.35/1.33	1.21/1.23

Tumor depth = 2 cm; breast thickness = 4.5 cm. Results are shown for CZT/Helix systems for each T/B ratio and average tumor diameter.

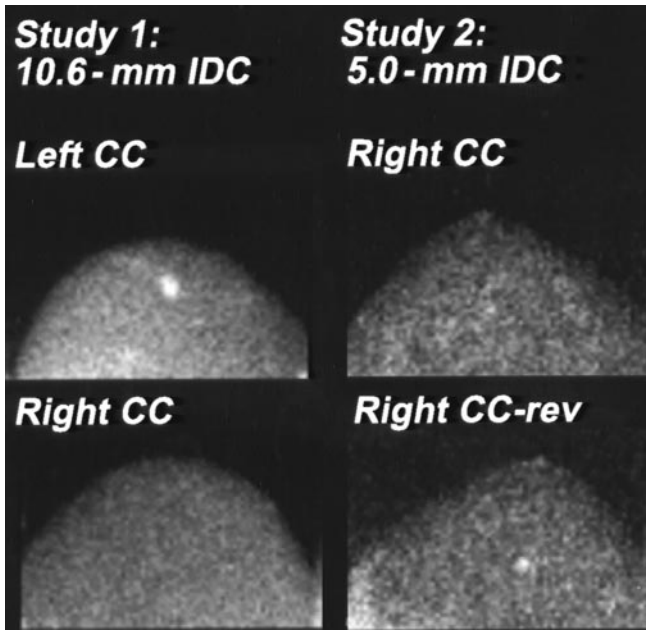

FIGURE 7. Example of clinical studies acquired on CZT detector. Craniocaudal (CC) and reverse craniocaudal (CC-rev) views show tumors of diameter 10.6 and 5 mm (confirmed at pathology) in 2 patients with invasive ductal carcinoma (IDC).

One of the limitations that is encountered in semiconductor detectors is energy tailing of events on the low-energy side of the photopeak (*7*) (Fig. 3). These events are caused by several factors, including incomplete charge collection for some photons and energy sharing between adjacent CZT pixels for photons that strike the detector at pixel boundaries. This tail makes it difficult to take advantage of the improved energy resolution of CZT (through use of a narrower energy window), because exclusion of these events from the energy window leads to a reduction in sensitivity and partly accounts for the reduced sensitivity of the CZT system relative to the Helix system. Despite this tailing problem, we anticipate some reduction in scatter content of images because scattered events will be preferentially degraded to lower energies and not up into the energy window. Majewski et al. (*1*) have found that scatter reduction or elimination is particularly important for the breast region closest to the chest wall. Reduction of the tail should improve energy resolution and permit use of a narrower energy window with reduction in scatter. Butler et al. (*8*) have demonstrated that, with innovative techniques for charge collection in CZT detectors, the magnitude of the tail can be

reduced, giving not only an improvement in energy resolution but also an improvement in sensitivity.

Proper alignment of the collimator holes to the individual CZT elements is a critical factor in obtaining optimal system resolution and minimal cross-talk between adjacent pixels. Slight misalignment between the collimator holes and the CZT elements was found to degrade extrinsic resolution measurements and result in the appearance of secondary peaks on extrinsic line spread function measurements. Many of these technical issues should be improved or resolved as this technology matures.

Optimal breast scintigraphy requires a detector that is capable of imaging the breast in an orientation similar to mammography. Conventional gamma cameras cannot be positioned in such a manner because of the large dead space at the edge of the detector. This dead space was measured at 8 cm on the Helix system and 10 cm on a Siemens Orbiter system, which makes it impossible to image the breast in a craniocaudal view, as with conventional mammography. By comparison, many of the pixilated scintillation systems (*1–6*) have dead spaces limited only by the shielding at the edge of the detector. The CZT detector used in this study had a dead space of 0.8 cm at the surface of the detector. It should be possible to further reduce this dead space because this detector was not designed or optimized for scintimammography. In addition, the use of an LB collimator moves this edge further away from the breast and should permit the posterior aspects of the breast to be included in the field of view. This feature, combined with its improved energy and spatial resolution, makes the CZT detector ideally suited for scintimammography. As would be expected from the system resolution measurements shown in Figure 4, the CZT system was better able to detect the simulated tumors in the breast phantom and had a higher contrast compared with a conventional gamma camera (Tables 1–4).

Although the improved performance of the CZT detector compared with the conventional NaI system is by itself relatively modest, it should be noted that it would be anatomically impossible for a conventional system to image the breast as we have done with this phantom model. In clinical studies, Scopinaro et al. (*11*) have reported that imaging of the breast in the prone position resulted in a breast thickness of ~16 cm, whereas imaging in the craniocaudal position with light (pain free) compression resulted in a breast thickness of 4–5 cm (*11*). This 3- to 4-fold reduction in breast thickness should significantly improve the ability of a gamma camera to detect smaller and deeper lesions. With a breast thickness of 4–5 cm, tumors will be a maximum of 2–3 cm from the collimator face. At this distance, the CZT detector offers a significant improvement (~1 mm) in spatial resolution compared with a conventional NaI detector (Fig. 4). Two large multicenter trials have shown that with prone imaging, scintimammography has a high sensitivity (75%–90%) for tumors >10–15 mm in diameter, but a poor sensitivity (40%–48%) for tumors <1 cm in diameter (*13,14*). Waxman et al. (*15*) reported that the mean diameter of lesions missed by scintimammography was ~9 mm. More recently, Lumachi et al. (*16*) obtained similar results and reported an average lesion size of 10.0 ± 3.5 mm for lesions missed by conventional scintimammography. In contrast to these results, a recent study by Brem et al. (*17*) using a small pixilated detector detected 10 of 15 lesions <1 cm in size compared with only 7 of 15 lesions detected by conventional scintimammography. This study supports our results presented in Tables 1–4 and in Figures 5–7 and indicates that scintimammography with a CZT system should perform significantly better than prone imaging with a conventional system for the detection of tumors <1 cm in diameter. In theory, a dual-detector CZT system coupled with light breast compression should further improve tumor detection (*1*) and may permit reliable detection of tumors as small as 5–7 mm in the breast.

We have recently started clinical trials with the CZT detector to ascertain the limits of tumor size that can be reliably detected with this type of device. Figure 7 illustrates the type of image quality obtained with this system in patients. These studies show 5- and 10-mm lesions well visualized in the breasts of 2 patients with invasive ductal carcinoma. It is of interest, however, that in the patient with the 5-mm lesion, the lesion was only seen on the reverse craniocaudal view. This would argue for the use of a dual-head detector system for optimal breast imaging.

In clinical practice, it is important that the breast tumor be both detected and accurately localized. In theory, this can be accomplished in several different ways. Several investigators have evaluated the potential of a dedicated SPECT system for breast imaging (*18,19*). One of the limitations of the current tomographic designs appears to be the long imaging time (1 h) required to obtain adequate image quality (*18*). Majewski et al. (*1*) compared planar versus SPECT imaging and concluded that planar imaging, with 2 opposing detector heads, while the breast is under compression yielded better visualization of small lesions than SPECT imaging. A dual-head system would allow an estimation of tumor depth from the ratio of counts from opposing detectors. The use of slant-hole collimators could be used to triangulate tumor position and depth. Finally, a combined scintimammography/mammography system may be useful for coregistration of the mammographic findings with those from scintimammography.

CONCLUSION

The imaging characteristics of a prototype CZT detector were evaluated for scintimammography. The detector exhibited improved energy and spatial resolution compared with a conventional gamma-camera system. Results in a phantom model showed significant gains in tumor detection, particularly for tumors 5–7 mm in diameter. The small dead space at the edge of the detector allows the device to be used in a similar manner to conventional mammography. The ability to position a CZT detector close to the breast as in

mammography, combined with the significant reduction in breast thickness compared with conventional scintimammography, should permit a CZT detector to reliably detect tumors <1 cm in size.

ACKNOWLEDGMENT

This work was supported by grants from General Electric Medical Systems and the Mayo Foundation for Education and Research.

REFERENCES

1. Majewski S, Kieper D, Curran E, et al. Optimization of dedicated scintimammography procedure using detector prototypes and compressible phantoms. *IEEE Trans Nucl Sci.* 2001;48:822–829.
2. McElroy DP, Hoffman EJ, MacDonald L, et al. Evaluation of breast tumor detectability with two dedicated, compact scintillation cameras. *IEEE Trans Nucl Sci.* 2002;49:794–802.
3. Pani R, Soluri A, Scafe R, et al. Multi-PSPMT scintillation camera. *IEEE Trans Nucl Sci.* 1999;46:702–708.
4. Gruber GJ, Moses WW, Derenzo SE, Wang NW, Beuville E, Ho MH. A discrete scintillation camera module using silicon photodiode readout of CsI(Tl) crystals for breast cancer imaging. *IEEE Trans Nucl Sci.* 1998;45:1063–1068.
5. Patt BE, Iwanczyk JS, Rossington Tull C, Wang NW, Tornai MP, Hoffman EJ. High resolution CsI(Tl)/Si-PIN detector development for breast imaging. *IEEE Trans Nucl Sci.* 1998;45:2126–2131.
6. Kim JH, Choi Y, Joo KS, et al. Development of a miniature scintillation camera using an NaI(Tl) scintillator and PSPMT for scintimammography. *Phys Med Biol.* 2000;45:3481–3488.
7. Takahashi T, Watanabe S. Recent progress in CdTe and CdZnTe detectors. *IEEE Trans Nucl Sci.* 2001;48:950–959.
8. Butler JF, Lingren CL, Friesenhahn SJ, et al. CdZnTe solid-state gamma camera. *IEEE Trans Nucl Sci.* 1998;45:359–363.
9. Eisen Y, Mardor A, Shor A, et al. NUCAM3: a gamma camera based on segmented monolithic Cd Zn Te detectors. *IEEE Trans Nucl Sci.* 2002;49:1728–1732.
10. National Electrical Manufacturers Association. *Performance Measurements of Scintillation Cameras*. NEMA Standards Publication NU 1-1994. Washington, DC: National Electrical Manufacturers Association; 1994.
11. Scopinaro F, Pani R, De Vincentis G, Soluri A, Pellegrini R, Porfiri LM. High-resolution scintimammography improves the accuracy of technetium-99m methoxyisobutylisonitrile scintimammography: use of a new dedicated gamma camera. *Eur J Nucl Med.* 1999;26:1279–1288.
12. Maublant J, de Latour M, Mestas D, et al. Technetium-99m-sestamibi uptake in breast tumor and associated lymph nodes. *J Nucl Med.* 1996;37:922–925.
13. Palmedo H, Biersack HJ, Lastoria S, et al. Scintimammography with technetium-99m methoxyisobutylisonitrile: results of a prospective European multicenter trial. *Eur J Nucl Med.* 1998;25:375–385.
14. Khalkhali I, Villanueva-Meyer J, Edell SL, et al. Diagnostic accuracy of ^{99m}Tc-sestamibi breast imaging: multicenter trial results. *J Nucl Med.* 2000;41:1973–1979.
15. Waxman A, Nagaraj N, Kovalevsky M, et al. Detection of primary breast malignancy with Tc-99m methoxyisobutylisonitrile (MIBI) in patients with non-palpable primary malignancies: the importance of lesion size [abstract]. *J Nucl Med.* 1995;36(suppl):194P.
16. Lumachi F, Ferretti G, Povolato M, et al. Accuracy of technetium-99m sestamibi scintimammography and x-ray mammography in premenopausal women with suspected breast cancer. *Eur J Nucl Med.* 2001;12:1776–1780.
17. Brem RF, Schoonjans JM, Kieper DA, Majewski S, Goodman S, Civelek C. High-resolution scintimammography: a pilot study. *J Nucl Med.* 2002;43:909–915.
18. Singh M, Mumcuoglu E. Design of a CZT based breast SPECT system. *IEEE Trans Nucl Sci.* 1998;45:1158–1165.
19. Wang H, Scarfone C, Greer K, et al. Prone breast imaging using vertical axis-of-rotation (VAOR) SPECT systems: an initial study. *IEEE Trans Nucl Sci.* 1997;44:1271–1276.